PROCEEDINGS of the
23rd International Congress on Acoustics

9 to 13 September 2019 in Aachen, Germany

# Assessing Engineered Materials via Non-Destructive Impact Acoustics

Yishan DONG; Shahram TAHERZADEH; David B SHARP; James BOWEN

School of Engineering and Innovation, The Open University, Milton Keynes, UK

## ABSTRACT

Acoustic testing allows inspection of the quality of engineered products without affecting their final use. It is an example of non-destructive testing (NDT), a wide group of analytical techniques used to evaluate the properties of a material, component or system without causing damage. Acoustic testing is becoming increasingly popular, particularly across the civil engineering, healthcare, automotive, and aviation industries. One early example originated via the wheeltappers during the Industrial Revolution when railways came into prominence. An impact between two solid bodies produces surface and body waves, the velocity and characteristics of which depend on material properties and the nature of the contact. Parameters such as density, modulus, and surface roughness influence the properties of these waves. Measurement of these waves can therefore be used in the evaluation of material and surface properties. This work reports on recent attempts to develop a non-destructive method for assessing the structure and quality of engineered materials. The protocol involves delivering a low kinetic energy impact to a sample, allowing correlation between the properties of the specimen and the specimen surface with the acoustic output from the impact event.

Keywords: impact, materials, roughness, surface

## 1. INTRODUCTION

There are many types of non-destructive testing (NDT) used in engineering, most of which have been developed as a means to monitor the condition of components, to undertake structure inspection, or to evaluate the physical properties of a material without causing any damage (1). Many traditional materials characterisation methods are partially or wholly destructive, carried out until the failure of a sample, in order to obtain physically meaningful information. For example, tensile testing is performed in order to obtain Young's modulus and yield stress. In general, a destructive testing (DT) method is easier to perform than a NDT method. DT results usually require less complex data processing post-acquisition. In most cases DT methods provide accurate results, but there are situations where DT is not possible or desirable; this is where NDT can offer a significant advantage, particularly when rare and/or expensive samples require consideration.

Acoustic NDT methods such as acoustic emission and ultrasound testing are becoming more and more popular in preventative maintenance strategies. During the Industrial Revolution, when railways came into prominence, a wheeltapper (2) was a person who would hit the train wheel with a long-handled hammer, listening carefully to the audible response. Experienced wheeltappers could use this method to diagnose cracks and wheel damage; these inspections helped to minimize downtime and keep companies ahead of their competitors. Acoustic NDT methods have come a long way since then, but the principle which underlies the wheeltappers' success is intrinsic to modern techniques.

Ongoing research regarding acoustic testing of materials includes investigation of physical properties such as porosity (3) and Young's modulus. The work presented here involves delivering a low kinetic energy impact to a specimen. The surface topography of the specimen will affect the mechanics of contact between the two impacting bodies. This will influence the squeezing of air out from between the two approaching bodies, and also the amount of air trapped between the bodies at the point of maximum deformation. Hence, it is anticipated that the acoustic output caused by the impact might also be influenced by surface topography of the specimen (4).

Surface topography is described by the surface roughness, a quantitative measure of the deviations (in the direction of the normal vector) of a real surface from its ideal form. If these deviations are large, then the surface is considered rough; if they are small, the surface is considered smooth (5). Surface roughness is important since it can predict the performance of a mechanical component. For example

in tribology, a rough surface wears out quickly due to higher friction, however roughness promotes oil adhesion. Surface topography is typically measured by a profilometer, which has high capital cost and requires specialist training. There are also usually size restrictions on the samples such instruments can accommodate.

The aim of the work presented here is to investigate the possibility of developing a new method of impact-based non-destructive testing. Such a technique could be used to define the physical characteristics of a specimen and the specimen surface.

## 2. EXPERIMENTAL

### 2.1 Materials

Aluminum sheet (AL104119, 99.5%H/H; Advent Research Materials, UK) was cut into plates of dimensions 100.0 mm × 100.0 mm × 2.0 mm. The Young's modulus of the aluminum, measured by tensile testing, was 70 GPa. The density of the aluminum was assumed to be 2,700 kg $m^{-3}$, and the average mass of each plate was measured to be 54 g. Solid nylon spheres of radius 6.25 mm were purchased from Dejay Distribution, UK; the density of the nylon was measured at 1,156 kg $m^{-3}$, each solid sphere having mass 1.2 g. The Young's modulus of the nylon was measured to be 1.21 GPa.

### 2.2 Profilometry

The surface topography of each Al plate and nylon sphere was measured using an optical profilometer (DCM3D, Leica Microsystems, UK). Six of the Al plates were roughened using different grades of SiC polishing paper, of grades P4000, P1200, P500, P240, P120 and P80 (Buehler, Germany). Each Al plate was roughened until a uniform surface was achieved. After polishing, the surface topography of each specimen was measured through a 10X lens. Five measurements were taken on each specimen, at non-overlapping locations. The average roughness of the surface, $S_a$ (6) was calculated using Mountainsmap software (Digital Surf, France) after performing a tilt correction.

### 2.3 Impact Event and Acoustic Recording

Impact events were generated by dropping a nylon sphere onto an Al plate to create a contact mechanism according to Hertzian mechanics (7). The plate was oriented perpendicularly to the direction of the approaching sphere, and was simply supported at all four corners. Although the results are not presented here, it should be noted that nylon spheres gave excellent repeatability of acoustic data when compared to other polymers tested; these were poly(propylene), poly(tetrafluoroethylene), poly(urethane), and viton. Fifty separate impact events were recorded.

The sphere radius, landing position, microphone position, and the initial height of the sphere above the Al plate, will all influence the acoustic data generated. In this work, the initial height of the sphere was 0.965 m, and the sphere was oriented above the centre of the Al plate. The microphone (SM 58 Vocal Microphone, Shure, USA) was held parallel to the Al plate surface; the tip of the microphone is approximately 5 mm from the plate edge. For each impact, the data was subsequently processed using Matlab (R2016b, MathWorks, USA) to obtain a sound spectrum. Specifically, the time domain data was processed via Fourier transform to obtain a frequency-vs-amplitude spectrum; the frequency range explored in this work is 0.40-20 kHz.

### 2.4 High Speed Load Cell

High speed recording of the force and duration of impact events was studied separately to acoustic recording. An Al plate was attached to a 10 N uniaxial load cell (TCA 720397, Procter and Chester Measurements, UK), shown in Figure 1. The load cell resonant frequency is approximately 1.0 kHz.

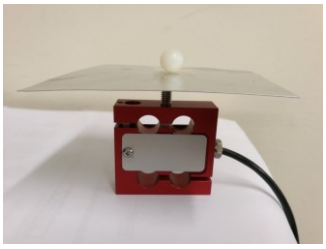

Figure 1: Load cell with attached aluminum plate; nylon sphere shown for scale

The analogue output from the load cell was collected by a DEWE-43A data acquisition instrument, connected to a desktop PC running DEWESoftX2 software (DEWESoft, Slovenia). The Al plate used for these measurements had dimensions 100.0 mm × 100.0 mm × 0.5 mm; the plate mass was 14 g, which meant that over 85% of the load cell range was available for measuring the impact force.

## 3. THEORY AND SIMULATION

### 3.1 Impact Energy

The nylon sphere is essentially in free fall through ambient air (21°C, 101.3kPa, humidity 20%), accelerating from zero velocity to its maximum velocity when it impacts the Al plate. The kinetic energy of the sphere, $E_k$, depends on the sphere mass, $m_{\text{sphere}}$, and its velocity, $v_{\text{sphere}}$:

$$E_{\text{k}} = \frac{m_{\text{sphere}} v_{\text{sphere}}^2}{2} \tag{1}$$

The sphere velocity at impact, when dropped from an initial height, $h$, of 0.965m, can be calculated according to:

$$v_{\text{sphere}} = (2gh)^{0.5} \tag{2}$$

where $g$ is gravitational acceleration of 9.81 m s$^{-2}$.

Given that the sphere has mass 1.2 g, and the impact velocity is 4.351 m s$^{-1}$, the kinetic energy at impact is 11.4 mJ.

### 3.2 Natural Frequency of a Solid Sphere

The natural frequency of a solid sphere, according to Lautrup (8), is given by:

$$\tan s = \frac{s}{\left(1 - \frac{s^2}{4q^2}\right)} \tag{3}$$

where $s$ is a dimensionless variable, and $q$ is the ratio between the transverse and longitudinal sound velocity in the material. The value of $q$ is 0.5 (9) for nylon.

Upon plotting equation 3, performed using MATLAB, the intersections between the curve and the x-axis are the solutions. The first solution, $s_1$, occurs at $s = 2.82$.

The speed of sound, $C_L$, under the experimental conditions employed in this work is 340 m s$^{-1}$.

The angular frequency of the sphere oscillation, $\omega_{\text{sphere}}$, is calculated using:

$$\omega_{\text{sphere}} = \frac{C_L s}{R} \tag{4}$$

where $R$ is the sphere radius, yielding $\omega_{\text{sphere},1}$ =153,408 rad s$^{-1}$ for $s_1 = 2.82$.

The angular frequency is converted to the natural frequency, $f_{\text{sphere}}$, according to:

$$f_{\text{sphere}} = \frac{\omega}{2\pi} \tag{5}$$

which gives the first mode of natural frequency of the nylon sphere as $f_1 = 24.032$ kHz.

Using Equations 3-5, the second solution is $f_{\text{sphere},2} = 48.087$ kHz, where $\omega_{\text{sphere},2}$ =301,984 rad, and $s_2 = 5.64$.

### 3.3 Natural Frequency of a Solid Plate

The natural frequency of a solid plate, $f_{\text{plate}}$, is given by (9):

$$f_{\text{plate}} = \frac{K_n}{2\pi}\left(\frac{Dg}{wd^4}\right)^{0.5} \tag{6}$$

where $K_n$ is a constant referring to the mode of vibration, $n$. The plate thickness is $d$, the load per unit area is $w$, and $D$ depends on the physical properties of the plate material:

$$D = \frac{E_{\text{plate}} d^3}{12(1 - \nu_{\text{plate}}^2)} \tag{7}$$

where $E_{\text{plate}}$ and $\nu_{\text{plate}}$ are the Young's modulus and Poisson's ratio of the plate respectively.

Assuming $\nu_{\text{plate}} = 0.33$ and $E_{\text{plate}} = 70$ GPa, Equation 7 gives $D = 52.37$ N m.

Values of $K_n$ are obtained from Roark's formulae (9) where $K_1$=19.7, $K_2 = K_3 = 49.3$.

The load per unit area is given by:

$$w = \frac{m_{\text{plate}} g}{A_{plate}} \tag{8}$$

where $A_{plate}$ is the cross-sectional area of the plate perpendicular to where load applies.

Therefore, $w = 52.974$ N m$^{-2}$, $f_{\text{plate},1} = 976.9$ Hz, and $f_{\text{plate},2} = 2.444$ kHz.

### 3.4 COMSOL Modelling

COMSOL Multiphysics software (COMSOL, UK) was employed for modelling the natural frequencies of both the nylon sphere and the Al plate. In each case a fine mesh 3D model was built for an Eigenfrequency study. Boundary conditions were selected to match the experimental conditions; four corners simply supported for the Al plate, and a fixed centre point for the nylon sphere. Material properties were imported from the COMSOL material library.

For the solid sphere, only three natural frequencies are predicted to be activated over the frequency range of interest in this work; 10.3 kHz, 10.4 kHz, and 10.7 kHz. In contrast, over fifty natural frequencies are predicted to be activated for the Al plate, ranging from 403 Hz to 24 kHz. Figure 2 shows examples of where and how the surface displacements are predicted to occur at specified natural frequencies. All of these calculated values are compared to the calculation results, and to the acoustic data, in order to interpret the acoustic impact event.

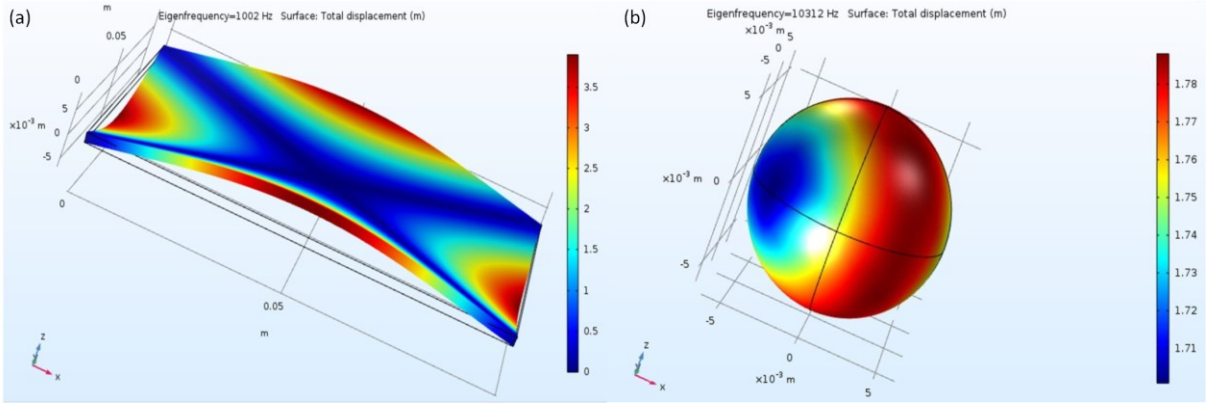


Figure 2: COMSOL simulation of surface displacement; (a) Al plate, natural frequency 1.0 kHz; (b) nylon sphere, natural frequency 10.3 kHz

## 4. RESULTS AND DISCUSSION

### 4.1 Surface Topography

The average roughnesses of the unpolished 'as-received' Al plate and the six polished Al plates are shown in Figure 3. The roughest surface, plate 6, achieved using P80 grade polishing paper, is approximately four times rougher than the surface of the unpolished plate. Plates 0-6 have thickness $d$ = 2.0 mm whereas Plates 7 and 8 have thickness $d$ = 0.5 mm and $d$ = 1.0 mm respectively.

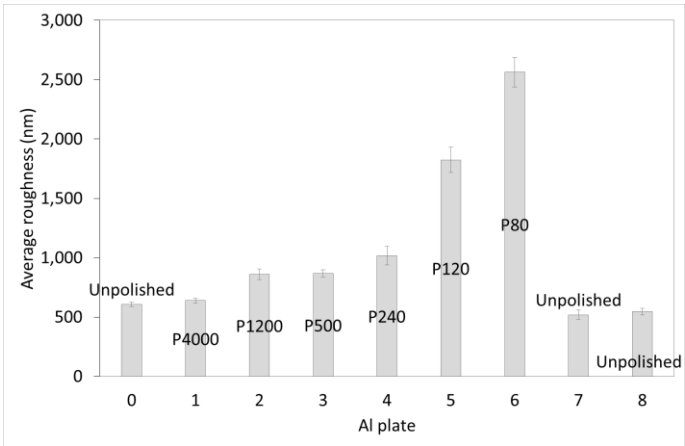


Figure 3: Average roughnesses of Al plate surfaces; error bars represent one standard deviation

## 4.2 Impact Mechanics

The load cell response from an example 'nylon-on-Al plate' impact event is shown in Figure 4. The mean time between the initial contact, point A, and the maximum normal load, point B, is 1.09 ± 0.05 ms. Point B is thought to be the point at which the rebound starts, and the nylon sphere begins to travel in the opposite direction to impact. i.e. upwards, away from the Al plate. The mean maximum normal load with which the nylon sphere impacts the Al plate is 8.64 ± 0.38 N.

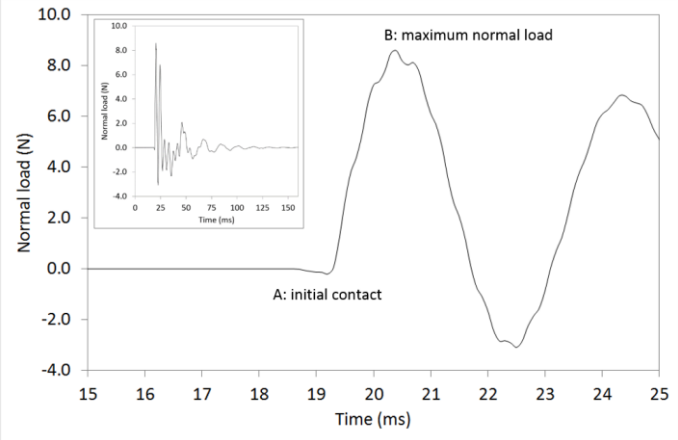


Figure 4: Load cell response for a nylon sphere impacting an Al plate

The contact area, a, between the sphere and plate and the vertical displacement of the sphere, $\delta$, are calculable according to Hertzian contact mechanics (7). It is assumed that the majority of deformation occurs in the nylon sphere, given it has a much lower modulus than the Al plate. The contact radius is given by (7, 10):

$$a = \left(\frac{RF}{k}\right)^{1/3} \tag{9}$$

where $F$ is the applied normal load, and $K$ is the effective elastic modulus, given by:

$$k = \frac{4}{3}\left(\frac{1-\nu_{\text{sphere}}^2}{E_{\text{sphere}}} + \frac{1-\nu_{\text{plate}}^2}{E_{\text{plate}}}\right)^{-1} \tag{10}$$

where $E_{\text{sphere}}$ and $\nu_{\text{sphere}}$ are the Young's modulus and Poisson's ratio of the sphere material respectively.

Further, the relationship between the vertical displacement, contact radius, and sphere radius is:

$$\delta = \frac{a^2}{R} \tag{11}$$

Assuming $\nu_{\text{sphere}} = 0.50$ (Poisson's ratio is dimensionless) and $E_{\text{sphere}} = 1.21$ GPa, at a maximum normal load of $F = 8.64$ N, Equations 9 and 10 give a maximum contact radius of $a = 0.268$ mm, while Equation 11 gives a maximum vertical displacement of $\delta = 13.9$ μm. It is useful to note that the contact pressure at the point of maximum normal load is on the order 30 MPa,

### 4.3 Impact Acoustics

Figure 5(a) displays time domain acoustic data for an impact event recorded when a nylon sphere impacts Plate 0, an unpolished Al plate. The acoustic event has a duration of approximately 70 ms, far longer than the time in which the impact and rebound event occurs according to the load cell data. Figure 5(b) illustrates how the data is transformed from voltage into sound pressure (by taking Fourier transform) and a linear trendline is fitted to the data. The gradient of the trendline is termed the 'decay constant'; the value of the decay constant for the data in Figure 5(b) is 71 log(Pa) $s^{-1}$.

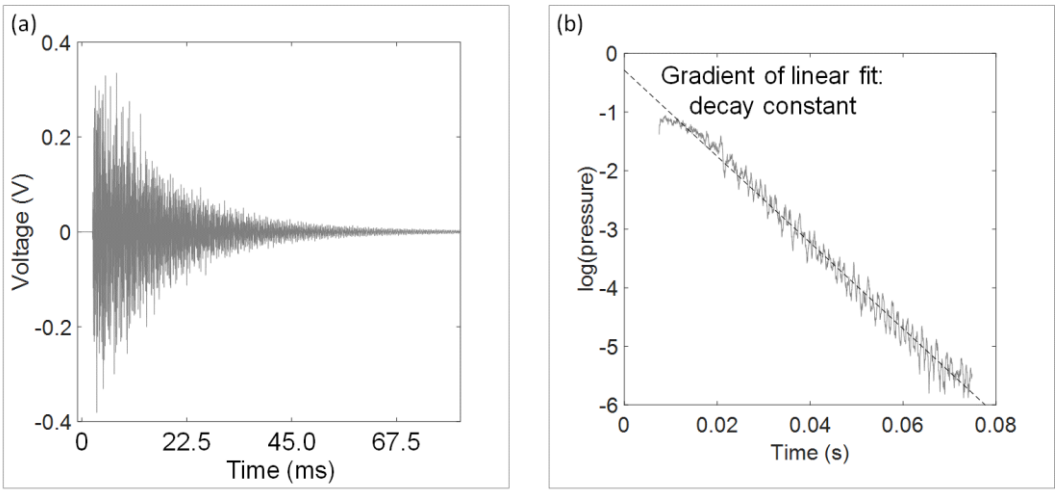


Figure 5: Acoustic data for nylon sphere impact on Plate 0; (a) voltage output from microphone, (b) calculating a decay constant for the sound pressure

Figure 6 illustrates the effect of surface topography and plate thickness on the impact acoustics. The decay constant increases with Al plate surface roughness, shown in Figure 6(a). This means that the acoustic event decays more rapidly as the plate topography becomes rougher. Figure 6(b) shows that the decay constant also increases with increasing plate thickness, which means that the acoustic response from an impact on an Al plate lasts longer for plates with lower mass, i.e. the plate vibrations are less damped.

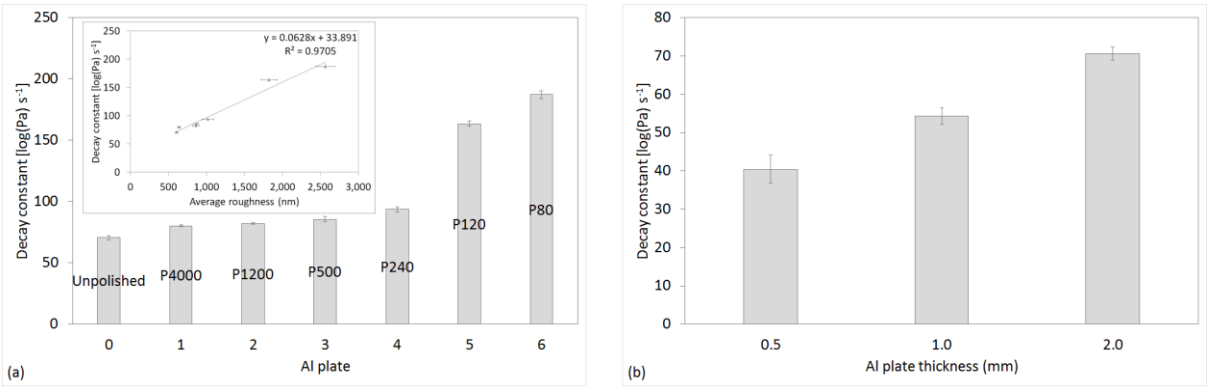


Figure 6: Decay constants for nylon spheres impacting on Al plates; (a) effect of surface topography, (b) effect of plate thickness

Figure 7 shows frequency-vs-pressure spectra for Plates 0, 1, 6, and 7, affording a visual comparison of the transformed acoustic outputs. Plates 0 and 7 are both unpolished, presenting surface topographies with similar roughness, but differ in their thickness, $d$ = 2.0 mm and $d$ = 0.5 mm respectively. Correspondingly, their acoustic spectra are markedly different, reflecting the difference in their acoustic output upon impact. Comparison of Plates 0 and 1, which exhibit similar thickness and surface roughness, Plate 1 having been roughened with grade P4000 polishing paper, demonstrates that a slight change in surface topography did not dramatically alter the acoustic spectra. Comparison of Plate 1 with Plate 6, a $d$ = 2.0 mm plate roughened with grade P80 polishing paper, illustrates that changing the surface roughness by a greater amount results in noticeably different acoustic spectra.

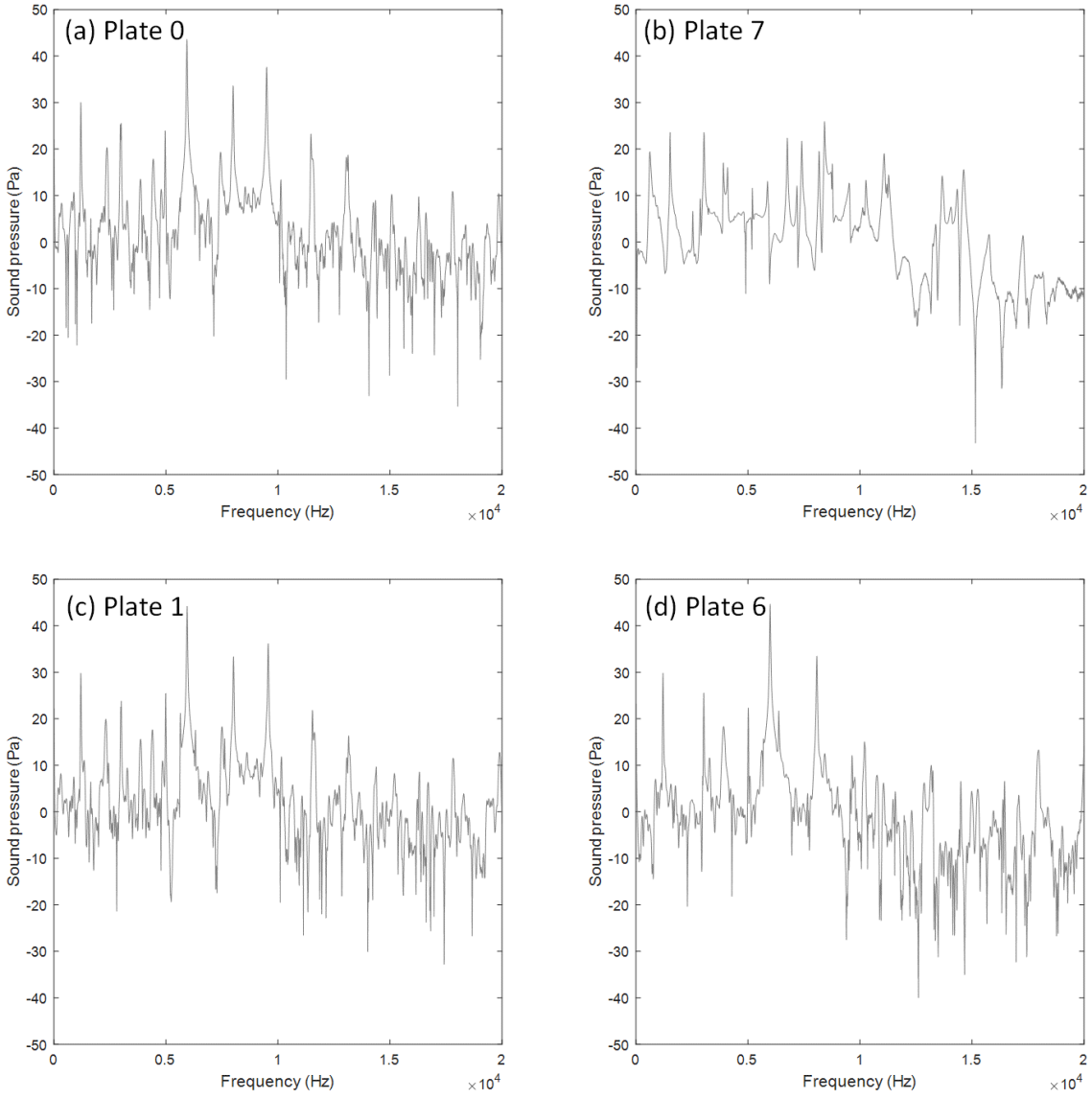


Figure 7: Acoustic spectra for a nylon sphere impacting Al plates: (a) $d$ = 2.0 mm, $S_a$ = 607 nm; (b) $d$ = 0.5 mm, $S_a$ = 547 nm; (c) $d$ = 2.0 mm, $S_a$ = 639 nm; (d) $d$ = 2.0 mm, $S_a$ = 2,564 nm

### 4.4 Comparison of Experiment, Theory, and Simulation

Comparison of the experimentally-acquired acoustic spectra in Figure 7 to theory and simulation does not reveal close alignment between predicted and measured frequency peaks. However, it should be noted that the calculated frequencies $f_{\text{plate},1} = 977$ Hz and $f_{\text{plate},2} = 2.444$ kHz match closely with the frequencies 978 Hz and 2.337 kHz predicted using COMSOL. This suggests that essential features of the plates and the impact event, which contribute strongly to the acoustic output, are absent from both the theory and the simulation. Investigating the critical parameters of the impact which

determine the magnitude and structure of the acoustic output is currently the subject of ongoing research.

## 5. CONCLUSION

This work sought to investigate the possibility of developing a new method of impact-based non-destructive testing, one which could be used to define the physical characteristics of a specimen and the specimen surface. The results presented in this paper demonstrate that the acoustic output from the impact of a nylon sphere on an aluminium plate can be used to determine differences in surface topography and plate thickness.

Processing and transformation of the recorded acoustic data was conducted in two ways. As a primary interpretation of the acoustic output from an impact event, the sound pressure was calculated whilst in the time domain, and a decay constant was calculated. This captures the rate at which the acoustic response from the impact event fades. By this method it was possible to determine differences in plate thickness and surface topography between samples. However, for some samples, use of this 'one dimensional' measure may not permit adequate discrimination between two or more changing physical properties.

Furthermore, a Fourier transformation was used to generate a spectrum in the frequency domain. By this method it was also possible to determine differences in plate thickness and surface topography between samples. This output was more time-consuming to generate, but yielded plots which serve as a useful 'two dimensional fingerprint' of the acoustic output from the impact event.

The acoustic spectra presented here are representative of the data collected from dozens of repeat measurements for the many sphere/plate combinations investigated. Future work will include the development of a method for assessing the similarity of acoustic spectra, so that the repeatability of a test can be captured and quantified using one, or perhaps two, unique parameters.

## ACKNOWLEDGEMENTS

The authors acknowledge the support and valuable contributions made by the following people: Damian Flack, Stan Hiller, Peter Ledgard, Peter Seabrook, and Alex Stronach.

## REFERENCES

1. Cartz L. Nondestructive Testing, ASM International. ISBN: 978-0-87170-517-4; 1995.
2. Railway Mission London. Railway signal: or, lights along the line. Palala Press. ISBN-13: 978-1347851388; 2015. Volume 9.
3. Shin H, Taherzadeh S, Attenborough K, Whalley W, Watts C. Non-invasive characterization of pore-related and elastic properties of soils in linear Biot–Stoll theory using acoustic-to-seismic coupling. European Journal of Soil Science; 2013.
4. Akay A. Acoustics of friction. The Journal of the Acoustical Society of America; 2002.
5. Zhai C, Gan Y, Hanaor D, Proust G, Retraint D. The Role of Surface Structure in Normal Contact Stiffness. Society for Experimental Mechanics; 2016.
6. Degarmo E Paul, Black J, Kohser Ronald A. Materials and Processes in Manufacturing (9th ed.). Wiley p223, 2003.
7. Hertz H.R, Ueber die Beruehrung elastischer Koerper. On Contact Between Elastic Bodies. Gesammelte Werke(Collected Works), , Leipzig. Germany; 1885; Vol. 1.
8. Lautrup B. Elastic vibrations. In B. Lautrup, Physics of Continuous Matter-Exotic and everyday phenomena in the macroscopic world. Copenhagen: The Niels Bohr Institute; 1998-2004; p. 212-222.
9. Young, W. Roark's Formulas for stress and strain. McGraw-Hill Book Company; 1989.
10. Johnson K. L. Contact mechanics. Cambridge University Press; 1985.